Concentrationdependent absorption and spontaneous emission of heavily doped GaAs

H. C. Casey and Frank Stern

Citation: J. Appl. Phys. **47**, 631 (1976); doi: 10.1063/1.322626
View online: http://dx.doi.org/10.1063/1.322626
View Table of Contents: http://jap.aip.org/resource/1/JAPIAU/v47/i2
Published by the American Institute of Physics.

Concentration-dependent absorption and spontaneous emission of heavily doped GaAs

H. C. Casey, Jr.

Bell Laboratories, Murray Hill, New Jersey 07974

Frank Stern

IBM Thomas J. Watson Research Center, Yorktown Heights, New York 10598

(Received 28 July 1975)

A model for the calculation of the absorption and emission spectra for GaAs at carrier concentrations in excess of 1×10^{18} cm^{-3} is described. This model utilizes a Gaussian fit to Halperin-Lax band tails for the concentration-dependent density of states and also includes an energy-dependent matrix element. The calculated absorption and emission spectra are compared to previous experimental results. All results are for 297 K. For p-type GaAs, the agreement is very good. The concentration dependence of the effective energy gap is obtained and can be expressed as E_g (eV) $= 1.424 - 1.6\times10^{-8}\,[p\ (\text{cm}^{-3})]^{1/3}$. The concentration-dependent thermal equilibrium electron-hole density product n_0p_0 and the radiative lifetime τ_r are calculated for p-type GaAs. The value of n_0p_0 increases from the low-concentration value of 3.2×10^{12} cm^{-6} to 1.2×10^{13} cm^{-6} at $p = 1.6\times10^{19}$ cm^{-3}. This value of n_0p_0, together with the thermal generation rate obtained from the experimental absorption coefficient, gives τ_r as 0.37 nsec at $p = 1.6\times10^{19}$ cm^{-3}.

PACS numbers: 78.50.G, 78.60., 71.55.F

I. INTRODUCTION

The high spontaneous emission quantum efficiency and the stimulated emission observed in the direct-gap III-V semiconductors have resulted in extensive studies of their properties, especially for GaAs. The influence of high impurity concentrations on the emission and absorption spectra has been well documented experimentally.[1-17] The present work was undertaken because of the availability of data for the optical absorption of impure GaAs[16] covering a wider photon energy range than most previous work. We have applied an approximate theoretical model for the density of states and the optical transition matrix element to the data because the model, unlike most theoretical treatments, can deal with the low-photon-energy range where impurity effects are important, with the high-photon-energy range where the conventional wave-vector selection rule applies, and with intermediate energies. The model had previously been used to calculate gain in compensated GaAs laser material,[18,19] and, with modifications, to calculate optical absorption in compensated Ge[20] and in amorphous Si.[21] This paper applies the model to optical absorption data for heavily doped GaAs, including p-type and n-type samples and a closely compensated Si-doped sample.

The theoretical model and the numerical evaluation are described in Sec. II. Experimental and calculated spectra are compared in Sec. III, and the reduction of the effective energy gap with concentration is obtained. The close agreement between experimental and calculated spectral shapes for heavily doped p-type GaAs ($p > 10^{18}$ cm^{-3}) permits evaluation of the concentration dependence of the radiative-recombination constant B, which is the optical generation rate divided by the electron-hole density product np, and of the radiative lifetime τ_r. In Sec. IV, numerical values are calculated for the equilibrium n_0p_0 in each sample and are combined with the thermal-generation rate deduced from the optical absorption to determine the rediative-recombination parameters. All results are for 297 K.

II. CALCULATION OF OPTICAL ABSORPTION

A. Introduction

Optical absorption in heavily doped semiconductors has been extensively studied theoretically,[22-28] but generally it has been possible to obtain quantitative results only in a narrow range of photon energies. In this section we calculate the absorption over a wide energy range, but at the expense of drastic approximations. In particular, we use a one-electron picture, omitting electron-hole Coulomb interaction[29-32] in calculating the magnitude of the optical absorption. Coulomb effects are taken into account approximately through their effect on the energy gap, as discussed in Sec. III.

In a one-electron model the optical absorption connected with transitions between a valence band and a conduction band can be written in the form[33]

$$\alpha(E) = (\pi e^2\hbar/\epsilon_0 m^2 c\bar{n}E) \times \int_{-\infty}^{\infty} \rho_c(E')\rho_v(E'')\,|M(E', E'')|^2[f(E'') - f(E')]\,dE', \tag{1}$$

where m is the free-electron mass, ϵ_0 is the permittivity of free space (replace ϵ_0 by $1/4\pi$ for cgs units), E is the photon energy, $E'' = E' - E$, $\bar{n}$ is the index of refraction at photon energy E, ρ_c and ρ_v are the densities of states per unit volume and unit energy in the conduction and valence bands, respectively, $f(E')$ is the probability that a state of energy E' be occupied by an electron, and M is the effective matrix element of the momentum operator between conduction-band states at energy E' and valence-band states at energy $E' - E$. When several valence bands are present, as for III-V semiconductors for which at least the heavy-hole and light-hole bands must be included, the total absorption coefficient is given by a sum of terms like Eq. (1) for each valence band.

Equation (1) assumes that the electrons are in quasi-equilibrium among themselves and the holes among

themselves. Several papers have invoked departure from quasiequilibrium to explain certain unexpected features of their results.[8,34–36] However, at room temperature for double heterostructures that ensure uniform excitation, the time-resolved spectra have the same spectral shape and shift in the same manner as the steady-state spectra. Therefore, the instaneous carrier density must have the same distribution as an equal density at steady state. This result demonstrates that quasiequilibrium exists within the conduction and valence bands.[37]

The approximations which have been used to find the density of states and the matrix element which enter in Eq. (1) are described in the following parts of this section.

B. Density of states

The density of states in semiconductors which are sufficiently heavily doped that the impurity levels have merged with the adjacent bands has been treated by many authors.[38–43] A model in which electrons have sufficiently low kinetic energy that they can follow the fluctuations in the potential leads, for Gaussian potential energy fluctuations whose root mean square is $V_{\rm rms}$, to a conduction-band density of states of the form[38]

$$\rho_c(E') = (2\eta_c)^{1/2}(m_{d,c}^{3/2}/\pi^2\hbar^3)y[(E' - E_c)/\eta_c], \tag{2}$$

where $m_{d,c}$ is the density-of-states mass, E_c is the nominal band edge of the conduction band, $\eta_c = \sqrt{2}V_{\rm rms}$, and

$$y(x) = \pi^{-1/2}\int_{-\infty}^{x}(x - z)^{1/2}\exp(-z^2)\,dz. \tag{3}$$

We call y the Kane function. The density of states in the valence band is given by an expression similar to Eq. (2) with the subscripted parameters replaced by the appropriate values for the valence band and with the sign of the argument of y changed.

If the potential fluctuations arise from the Coulomb potentials of N_D^+ ionized donors and N_A^- ionized acceptors per unit volume, randomly located, then the rms potential energy fluctuation is[38,44]

$$V_{\rm rms} = (e^2/4\pi\epsilon)[2\pi(N_D^+ + N_A^-)L]^{1/2}, \tag{4}$$

where ϵ is the permittivity and L is the screening length, given by

$$L = \left[-\left(\frac{d\rho}{d\varphi}\right)_{\varphi=0}\epsilon^{-1}\right]^{-1/2}, \tag{5}$$

where ρ is the charge density in the crystal and φ is the electrostatic potential associated with the presence of the charged impurities. In general, L depends on the carrier concentration, on the temperature, and on the shape of the density of states.

The density of states given in Eq. (2) makes no allowance for electron tunneling through potential barriers, and therefore overestimates the extent of the band tailing unless the carriers have a very large effective mass. The kinetic energy of the carriers was taken into account in the work of Halperin and Lax,[40] who gave numerical results for the density of states in a limited energy range in the band tail. The extent to which kinetic energy effects reduce band tailing depends on the "kinetic energy" $\hbar^2/2m^*L^2$ in relation to the rms potential fluctuations.[22,43,45,46]

We approximate the density of states by fitting a one-parameter density of states of the Kane form to the Halperin-Lax results in the band tail, and use the bulk density-of-states mass to assure that the density of states agrees with the value in the undisturbed crystal for energies well above the band tail. Other authors[47–49] have used slightly different ways to interpolate between the Halperin-Lax tail and the unperturbed density of states. Our only parameter is the band-tailing energy η, which is found by requiring that the approximate density of states equal the value given by Halperin and Lax at the energy where $b(\nu) = 10\xi'$ in their notation,[40] an energy within the range of validity of their results. An example of the fit is shown in Fig. 1. The other samples discussed in this paper lead to similar results except that the approximate density of states lies even closer to the Halperin-Lax curve than for the case shown in Fig. 1.

To the best of our knowledge, no theory of the effect of fluctuations on band tailing has taken the detailed structure of the energy bands into account, but has assumed isotropic, nondegenerate, parabolic bands. In making the calculations for GaAs we have taken the nonparabolicity of the conduction band into account by replacing the mass at the bottom of the conduction band, for which we use $m_c = 0.066m$, by a slightly larger mass characteristic of the energy of a typical electron. The correction is of order 10% or less and does not have significant effect on our results. A similar procedure was followed for the light-hole band, for which we used $m_{\rm lh} = 0.085m$. The heavy-hole mass was taken to be $0.55m$.

The screening length L which enters in finding the Halperin-Lax density of states depends on the form of the density of states implicitly through Eq. (5). The

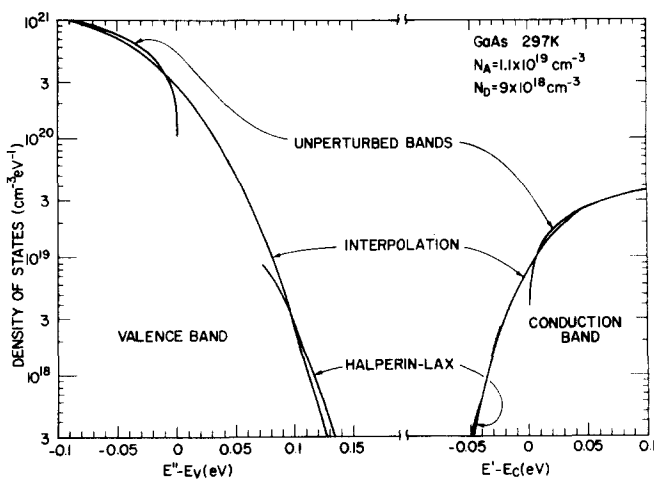

FIG. 1. Densities of states in the conduction and valence bands for GaAs with 2×10^{18} net acceptors per cm^3. The upper curves show the densities of states in the unperturbed bands, the lower curves show the densities of states in the band tail as calculated from the theory of Halperin and Lax, and the curves which join them are the interpolated Kane functions used as the densities of states in our calculation.

TABLE I. Energy band parameters for p-type GaAs at 297 K. $F_p' = F_p - E_v$ is the hole quasi-Fermi level relative to the nominal valence band edge: η_c and η_v are the band-tail parameters for the conduction and valence bands, respectively.

p (cm^{-3})	Impurity	Mobility (cm^2/V sec)	N_A (cm^{-3})	N_D (cm^{-3})	E_g (eV)	η_c (meV)	η_v (meV)	Screening length (Å)	V_{rms} (meV)	F_p' (meV)
1.2×10^{18}	Zn	162	1.5×10^{18}	3×10^{17}	1.408	10	20	39	23	59
2.4×10^{18}	Zn	102	3×10^{18}	6×10^{17}	1.403	9	22	28	28	40
1.6×10^{19}	Zn	67	2×10^{19}	4×10^{18}	1.381	5.5	29	13	49	−20
Si-A			6×10^{18}	4×10^{18}	1.404	23	43	30	48	56
Si—2×10^{18}	Si	35								
Si-B			1.1×10^{19}	9×10^{18}	1.404	37	61	29	67	70

calculation was therefore carried out self-consistently. But at room temperature the density of states has relatively little influence on L, so the free-carrier result (Debye length) $L = (\epsilon KT/pe^2)^{1/2}$ could have been used with little error.

We use the same value of the band-tail parameter η for both the light- and heavy-hole bands. The light-hole band must be included in the optical absorption calculation because it contributes about one-third of the absorption in lightly doped samples and affects the absorption edge in heavily doped samples. The split-off valence band is ignored because it makes no significant contribution to the optical absorption of GaAs in the energy range of interest here.

Values of the parameters obtained by the procedure we have just described are listed in Table I for the p-type samples considered in this work. The assignment of the other quantities in Table I is discussed in Sec. III.

C. Optical matrix element

Several approximations are available for finding the matrix element which enters in the optical absorption coefficient α. In undoped III-V semiconductors, α can be obtained from the theory of Kane,[50] who used a band structure model that includes both nonparabolicity and warping. He dealt with material for which the wave-vector selection rule, which ignores the small wave vector of the photon and requires initial and final states to be at the same wave vector, is used. The opposite extreme, useful in a limited range of energies near the energy gap, is to suppose that the matrix element is constant, independent of the energy of initial and final states. As we shall show in Sec. III, the constant-matrix-element approximation leads to grossly unphysical results when the photon energy is beyond the band-tail region. On the other hand, the k-selection rule cannot be applied in the band tail, where potential fluctuations destroy the translational symmetry of the crystal and deform the eigenfunctions so they no longer resemble plane waves.

For localized states, the wave function can be written in effective mass approximation in the form $\psi = \psi_{env}(\mathbf{r})u(\mathbf{r})$, where u is a Bloch function at the appropriate band edge and ψ_{env} is a normalized envelope function. For a plane-wave state with wave vector $\mathbf{k}$, the wave function can be written in the form $\psi = V^{-1/2}u(\mathbf{r}) \times \exp(i\mathbf{k}\cdot\mathbf{r})$, where V is the volume of the system. The dipole matrix element for transitions between a localized state in one band and a plane-wave state in another band is then given approximately by

$$M = M_b M_{env}, \tag{6a}$$

$$M_{env} = V^{-1/2}\int \psi_{env}^*(\mathbf{r})\exp(i\mathbf{k}\cdot\mathbf{r})d^3\mathbf{r}, \tag{6b}$$

where M_b is an average matrix element connecting Bloch states near the band edges. For III-V semiconductors we use

$$|M_b|^2 = \frac{m^2P^2}{6\hbar^2} \approx \frac{m^2E_g}{12m_c}\,\frac{E_g+\Delta}{E_g+\frac{2}{3}\Delta}\ , \tag{7}$$

where P is the interband matrix element used by Kane,[50] E_g is the energy gap, and Δ is the spin-orbit splitting. A factor $\frac{1}{3}$ arises in Eq. (7) from an average over all directions, and a factor $\frac{1}{2}$ arises from the spin selection rule. For GaAs we use the value of m_c given above, $\Delta = 0.33$ eV, and $E_g = 1.424$ eV and find that $|M_b|^2 = 1.35mE_g$. Corrections to this value which arise from thermal effects and from contributions of higher bands to the effective mass at the bottom of the conduction band have been ignored.

When the localized state wave function is assumed to have a hydrogenic form, the envelope matrix element in Eq. (6b) reduces to the form given by Eagles[51]:

$$|M_{env}|^2 = 64\pi a^{*3}(1 + a^{*2}k^2)^{-4}V^{-1}, \tag{8}$$

where $a^* = 4\pi\epsilon\hbar^2/m^*e^2$ is the effective Bohr radius of the localized state.

The envelope matrix element which we use to calculate the optical absorption for impure GaAs is an *ad hoc* matrix element chosen to have the correct limiting behavior at high photon energy, where the k-selection rule applies, and for transitions between localized states and plane-wave states. It is derived by assuming that the envelope wave function has the form

$$\psi_{env} = (\beta^3/\pi)^{1/2}\exp(i\mathbf{k}\cdot\mathbf{r})\exp(-\beta|\mathbf{r}-\mathbf{r}_i|), \tag{9}$$

where β characterizes the localization of the state, $\mathbf{r}_i$ is the point at which it is centered, and $\mathbf{k}$ is a measure of its plane-wave character.

To calculate the parameters $\mathbf{k}$ and β for the *ad hoc* envelope wave function for a state of energy E' in the perturbed conduction band, we define another energy E^* such that the number of states at energies less than E^* in the unperturbed density of states equals the number of states at energies less than E' in the actual density of states. Then $E^* - E'$ is a measure of the lower-

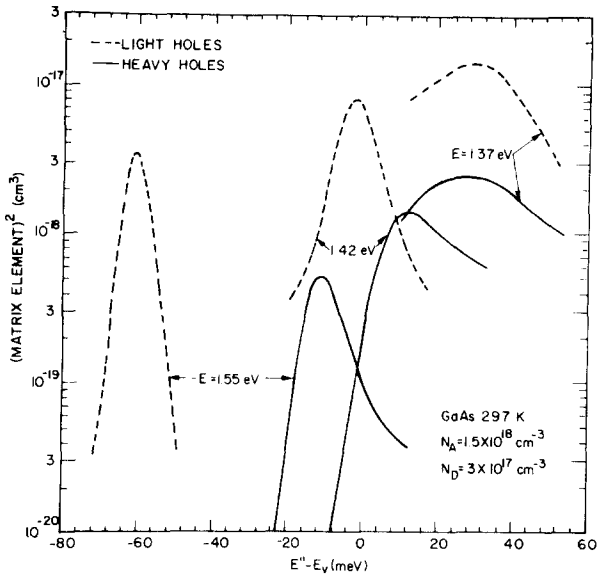

FIG. 2. Envelope matrix element for optical transitions between valence and conduction bands of GaAs with 1.2×10^{18} net acceptors per cm^3 for three photon energies, vs the energy of the initial state in the valence band. Note that there are two sets of results, for transitions from the heavy-hole band and for transitions from the light-hole band.

ing of the energy by potential fluctuations. We now define

$$\hbar^2 k_c^2/2m_{d,c} = E^* - E_c, \tag{10a}$$

$$\hbar^2 \beta_c^2/2m_c^* = h_c(E^* - E'), \tag{10b}$$

where E_c is the nominal conduction band edge. The factor h_c is chosen to make $h_c(E^* - E')$ equal the kinetic energy of localization, T,[40] for a state at the energy where our density of states is fitted to the Halperin-Lax value. The density-of-states mass m_d and the susceptibility mass m^* are essentially the same in our calculation.

At high energies, where $E^* \approx E'$, we recover the usual plane-wave result. At low energies, where $E^* \approx E_c$, the state is localized and has the appropriate kinetic energy of localization. For intermediate energies the wave function of Eq. (9) may differ significantly from the correct envelope function.

The envelope matrix element is the product of the complex conjugate of the wave function of Eq. (9) and a corresponding wave function for the valence band, averaged over all directions of the wave vectors and over all positions of the sites at which the states are localized. We then find

$$|M_{\rm env}|^2 = (64\pi b/3)(t^4 - q^4)^{-5}[(b^4 - 5b^2B^2 + 5B^4)(3t^4 + q^4)(t^4 - q^4) + 8b^2B^2t^2(3b^2 - 10B^2)(t^8 - q^8) + 16b^4B^4(5t^8 + 10t^4q^4 + q^8)], \tag{11}$$

where $B = \beta_c\beta_v$, $b = \beta_c + \beta_v$, $t^2 = b^2 + k_c^2 + k_v^2$, and $q^2 = 2k_ck_v$.

The structure of the matrix element is shown in Fig. 2, where $|M_{\rm env}|^2$ is plotted as a function of the energy of the valence-band state from the nominal valence-band edge for three different photon energies. There are two sets of curves, one for transitions from the heavy-hole band and one for transitions from the light-hole band. Note that the matrix element is rather flat for the lowest photon energy, not so different from the constant matrix element often used in this energy range.

It is not hard to show that for photon energies for which the k-selection rule should be valid or nearly valid, the matrix element $M_{\rm env}$ should peak where

$$E_v - E'' = (m_c/m_v)(E' - E_c) = m_c(E - E_g)/(m_c + m_v), \tag{12}$$

and its integral should be

$$\int_{-\infty}^{\infty} |M_{\rm env}(E', E' - E)|^2 dE' = \pi^2\hbar^3/[\tfrac{1}{2}m_cm_v(m_c + m_v)(E - E_g)]^{1/2} \tag{13}$$

if parabolic bands with effective masses m_c and m_v are assumed.

We have verified that the *ad hoc* envelope matrix element satisfies Eq. (13) for transitions from the light-hole band when $E = 1.55$ eV, the only case in Fig. 2 that is not significantly influenced by band tailing. In addition, when $\beta_c = 0$ and $k_v = 0$, the envelope matrix element effectively reduces to Eq. (8).

The prescription described in this section has been used to calculate the optical absorption and gain, and the spontaneous emission, for impure GaAs[18,19,52] and, with modifications for the change in band structure, for amorphous Si.[21] One of the purposes of the present work is to assess the adequacy of the interpolation procedure which this matrix element provides.

III. ABSORPTION AND EMISSION SPECTRA

A. p-type GaAs

The properties of the Zn-doped melt-grown (MG) samples and the Si-doped liquid-phase epitaxy (LPE) sample used for the comparison of the experimental and calculated absorption and emission spectra are summarized in Table I together with the band-tail parameters derived in Sec. II. The assignments of E_g will be described later in this section. The free hole concentration p and mobility at 297 K were determined by Hall measurements. Only samples with $p \gtrsim 1\times10^{18}$ cm^{-3} were considered because the band-tail model used in Sec. II is invalid at lower doping levels. Hall measurements show that the acceptor ionization energy goes to zero at a hole concentration between 1×10^{18} and 5×10^{18} cm^{-3}.[53] The assignment of the acceptor concentration N_A and the donor concentration N_D for a given hole concentration is difficult, and different considerations are required for the Zn- and Si-doped samples.

As shown in Table I, the ratio N_A/N_D was taken as 5.0 for the Zn-doped samples. This value was based on the results of previous studies of Zn-doped GaAs by Ermanis and Wolfstirn.[53] In the concentration range considered here, they gave hole concentrations that were obtained from Hall measurements and corresponding Zn concentrations that were determined by neutron activation. At these concentrations, the Zn acceptors are fully ionized so that $N_A - N_D = p$, and for $p = 1.1\times10^{18}$ and 3.7×10^{18} cm^{-3}, $N_A/N_D \approx 5.0$.[53]

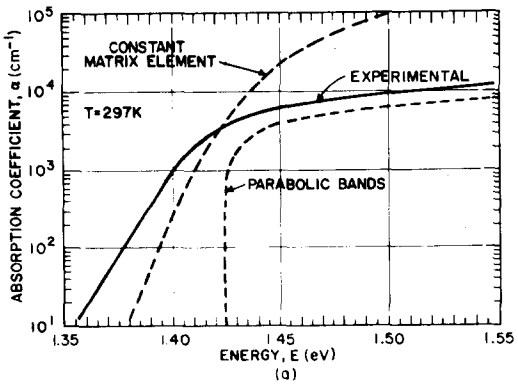

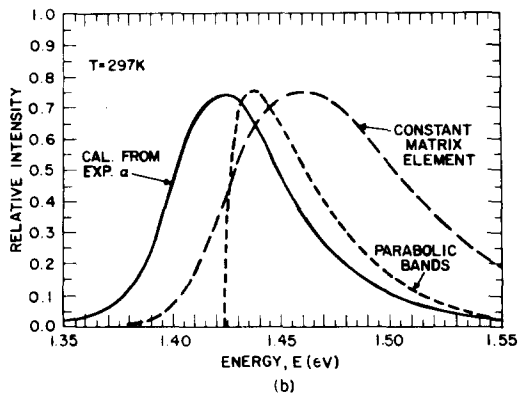

FIG. 3. (a) Comparison of experimental absorption coefficient for $p = 1.2 \times 10^{18}$ cm^{-3} (Ref. 16) with α calculated for a parabolic density of states and for a density of states with band tails but a constant matrix element. (b) Spontaneous emission spectra deduced from the absorption curves in (a) using detailed balance. The curves have been normalized to the same peak height.

The hole concentration for the Si-doped sample was determined by growing a Si-doped layer on a Cr-doped substrate with LPE. Solid-state mass spectrometry measurements[54] on Si-doped LPE layers gave a total Si concentration of $3 \pm 1 \times 10^{19}$ cm^{-3}. Measurements of Si-localized vibrational modes[55] have shown the presence of Si donors, acceptors, and neutral Si. Therefore, the Si-A entry in Table I was chosen to given a $N_A + N_D$ of 1×10^{19} cm^{-3}, while the Si-B entry is for $N_A + N_D$ of 2×10^{19} cm^{-3}. A more precise assignment of N_A and N_D for the LPE Si-doped sample is not possible at the present time.

The energy gap E_g as a function of hole concentration was determined by the value of E_g that gave the best agreement between the experimental absorption edge and the values calculated from the model described in Sec. II. The assignment of E_g has no influence on the spectral shape, only on the position.

The experimental absorption coefficient that was obtained in Ref. 16 for the sample in Table I with $p = 1.2 \times 10^{18}$ cm^{-3} is shown in Fig. 3(a). The free-carrier absorption has been removed. Two calculated curves are also indicated by the dashed lines. A model with the usual parabolic-band density of states, a direct-transition matrix element, and $E_g = 1.424$ eV gives an absorption coefficient marked "parabolic bands" that has very little resemblance to the experimental α below 1.45 eV. The constant-matrix-element curve uses the band-tail parameters of Table I, but a constant matrix element. The assumption of a constant matrix element leads to an α that greatly exceeds the experimental value for $E > E_g$.

In Fig. 3(b), the emission spectra are compared. The curves are calculated from α using the detailed-balance approach of van Roosbroeck and Shockley[56] which gives the equilibrium emission intensity $\mathcal{J}(E)$ at photon energy E as

$$\mathcal{J}(E) = \frac{8\pi \bar{n}^2 E^2 \alpha(E)}{h^3 c^2 [\exp(E/kT) - 1]}, \tag{14}$$

where $\alpha(E)$ is the absorption coefficient at the energy E. The relative peak intensities in Fig. 3(b) have been normalized to the same peak intensity to permit comparison of the spectral shapes. Neither the parabolic-band case or the constant-matrix-element case agrees with the spectrum calculated from the experimental α by Eq. (14).

In Fig. 4(a), the calculated absorption coefficient

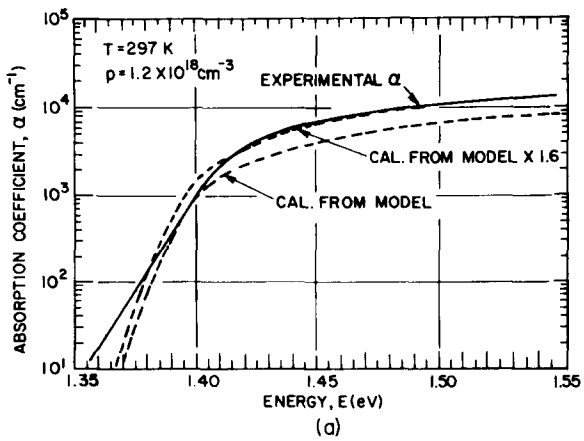

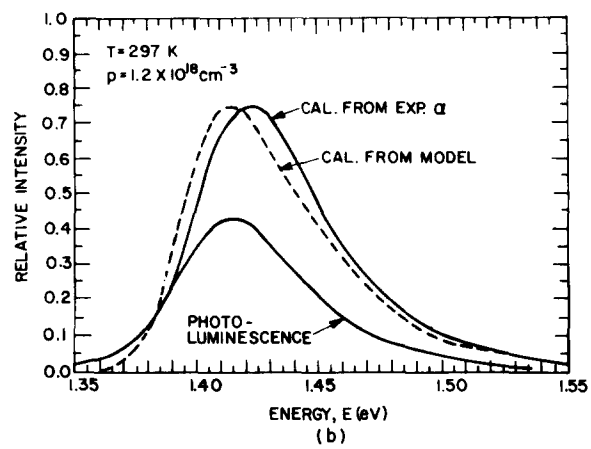

FIG. 4. (a) Comparison of the experimental (Ref. 16) and calculated absorption coefficients for $p = 1.2 \times 10^{18}$ cm^{-3}. The effective energy gap used in the calculated absorption coefficient is taken from Eq. (15). (b) Comparison of the emission spectrum calculated with the experimental α in Eq. (14) and the spectrum calculated from the model. The experimental photoluminescence emission spectrum is also shown.

utilizes both the band-tail parameters of Table I and the matrix element of Eq. (11) in Eq. (1). The experimental α and hole concentration are the same as for Fig. 3. The calculated α closely reproduces the shape of the experimental absorption, but the absolute calculated absorption strength is too small by a factor of ~1.6 at the higher photon energies. The curves diverge at low α, which indicates that the density of states deep in the band tails, or the matrix element at low energy, is somewhat too small or that other broadening mechanisms are present.

In Fig. 4(b), the emission spectra are compared. These spectra were obtained from the experimental and calculated absorption coefficients by Eq. (14).

To provide a self-consistency check on the emission spectral shapes, the photoluminescence spectrum was measured for the same sample used to determine the experimental α. The sample was excited with the 1.916-eV line of a krypton laser, and the measured spectrum was corrected for spectrometer and photomultiplier energy dependence. The photoluminescence spectrum has been normalized in intensity to agree at low energy with the spectrum calculated from the experimental absorption coefficient. Because of self-absorption, the photoluminescent peak intensity should be reduced and shifted to lower energy. The relationship between the internal emission spectrum represented by the "calculated from experimental α" curve and the observed photoluminescent curve has been given by Williams and Chapman[57] and Hwang.[13] At this excitation energy α is 3.8×10^4 cm^{-1}.[58] With the experimental α of Fig. 4(a) in the expressions of Refs. 57 or 13, agreement between the photoluminescent spectrum and the spectrum calculated by Eq. (14) is obtained for a minority-carrier diffusion length L_n of 2 ± 0.5 μm. Previous measurements of L_n for Ge-doped LPE layers gave $L_n\approx5$ μm for this hole concentration.[59] This shorter diffusion length for the Zn-doped melt-grown sample is consistent with the lower photoluminescent intensity of the melt-grown sample as compared to the LPE sample. Therefore, the spectrum calculated from the experimental absorption coefficient is consistent with the independent photoluminescent measurement.

The calculated absorption coefficients calculated for all three Zn-doped samples are shown in Fig. 5(a), and for comparison the experimental[16] absorption coefficients for the same hole concentrations are shown in Fig. 5(b). In all cases, the calculated α decreases too rapidly at low energy and the absorption strength is too weak by a factor of approximately 1.5—2.1. However, all the essential features are obtained for the calculated absorption coefficients. The calculated absorption coefficient below 10^3 cm^{-1} moves to lower energy as p increases, and the absorption coefficient at 1.55 eV becomes smaller as p goes to 1.6×10^{19} cm^{-3}.

In Table II, the peak positions and half-widths for the emission spectra are compared for measured photoluminescence (uncorrected for self-absorption), the spectra calculated from the experimental α, and the spectra calculated from the model of Sec. II. For the Zn-doped samples, the spectra obtained from the experimental α and from the model agree within 0.01 eV

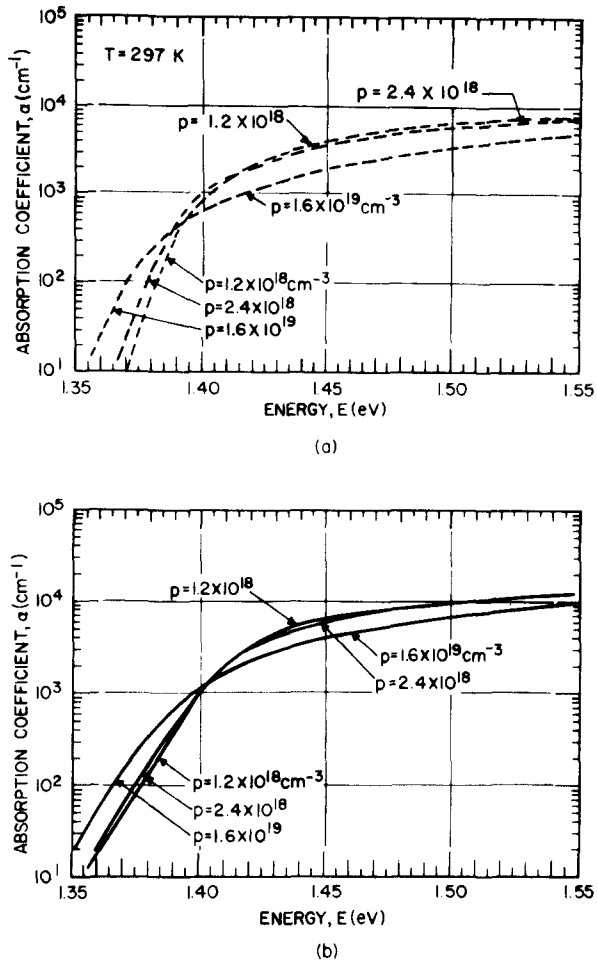

FIG. 5. (a) Absorption coefficient calculated for the indicated hole concentrations. The effective energy gap used in the calculated absorption coefficient is taken from Eq. (15). (b) Experimental absorption coefficient for the indicated hole concentrations (Ref. 16).

in peak position and within 0.002 eV in half-width. The photoluminescent peak position is lower in energy, as it should be due to self-absorption. The disagreement in spectral shape is at low energy as illustrated in Fig. 4(b). The Si-doped sample summarized in Table II will be considered in detail later in this section.

The energy gap shrinkage given in Table I was obtained by the best fit between the calculated and measured absorption edges. The fit was carried out in two ways. One way assumed that the Coulomb enhancement factor found at high photon energies persisted through the absorption edge region. The other fit assumed that the enhancement factor approaches unity in the absorption tail.[31] The energy gap given in Table I is the average of the two values.

For high-purity GaAs, the energy gap at 297 K is 1.424 eV.[60] The energy gap shrinkage is taken as the difference of 1.424 eV and the value of E_g given in Table I. The resulting energy gap shrinkage ΔE_g is plotted in Fig. 6 with an uncertainty of ±0.003 eV for the two lower dopings, and ±0.005 eV for the highest doping. The data show a variation as $p^{1/3}$ and may be represented by

TABLE II. Properties of emission spectra for p-type GaAs at 297 K.

p (cm^{-3})	Photoluminescence		Peak position		Half-width	
	Peak position (eV)	Half-width (eV)	Calc from α (eV)	Calc from model (eV)	Calc from α (eV)	Calc from model (eV)
1.2×10^{18}	1.415	0.059	1.425	1.414	0.063	0.063
2.4×10^{18}	1.415	0.061	1.420	1.411	0.065	0.064
1.6×10^{19}	1.400	0.070	1.405	1.398	0.073	0.074
Si-A	• • •	• • •	• • •	1.387	• • •	0.084
Si—2×10^{18}	1.375	0.098	1.380	• • •	0.105	0.104
Si-B	• • •	• • •	• • •	1.352	• • •	0.105

$$E_g\ (\text{eV}) = 1.424 - 1.6\times10^{-8}p^{1/3}, \tag{15}$$

with p in units of cm^{-3}. The energy gap shrinkage is discussed in Sec. V.

The results for the Si-doped sample are shown in Fig. 7. Silicon is an amphoteric impurity in GaAs and, in samples prepared by liquid-phase epitaxy, close compensation and high luminescent efficiency result. External quantum efficiencies of 20% are obtained for Si-doped electroluminescent diodes[61] and the lowest reproducible normalized laser threshold $J_{th}/d = 4.0$ kA/cm^2 μm, where d is the active layer thickness, is obtained with Si-doped active layers.[62] The experimental α for the Si-doped case was obtained with a sample configuration in which GaAs is the central layer of a three-layered $Al_xGa_{1-x}As$-GaAs-$Al_xGa_{1-x}As$ structure (see Fig. 1 of Ref. 58). For $\alpha \gtrsim 5\times10^2$ cm^{-1}, the absorption coefficient was obtained from the photoluminescence spectrum of the thin layer by Eq. (11) of Ref. 58.

The absorption and emission spectra calculated from the model of Sec. II are shown for two cases in Fig. 7 (see Table I). The energy gap was assigned from Eq. (15) for a hole concentration of 2×10^{18} cm^{-3}. The Si-A case of $N_A + N_D = 1\times10^{19}$ cm^{-3} in Fig. 7(a) drops too sharply at low energy as compared to the experimental α in Fig. 7(a), while the Si-B of $N_A + N_D = 2\times10^{19}$ cm^{-3} case decreases too slowly at low energy. In Fig. 7(b) the emission spectrum calculated by the model of Sec. II for Si-A is too narrow and has an emission intensity about 0.010 eV above the peak of the spectrum calculated from the experimental α by Eq. (14). For the Si-B case, the spectral shapes agree quite closely, but the energy of the peak emission intensity for the spectrum calculated from the model is about 0.020 eV below the peak calculated from the experimental α. These two cases illustrate how quickly the spectral peak position shifts as $N_A + N_D$ is varied for this case of close compensation.

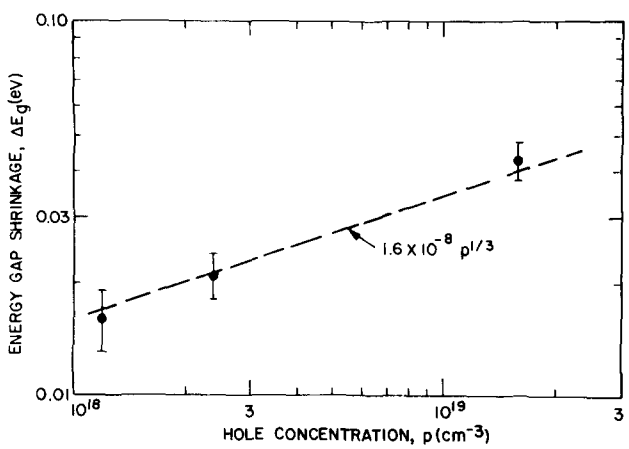

FIG. 6. Concentration dependence of the effective energy gap shrinkage.

B. n-type GaAs

The Te-doped melt-grown samples used for the comparison of the experimental and calculated absorption

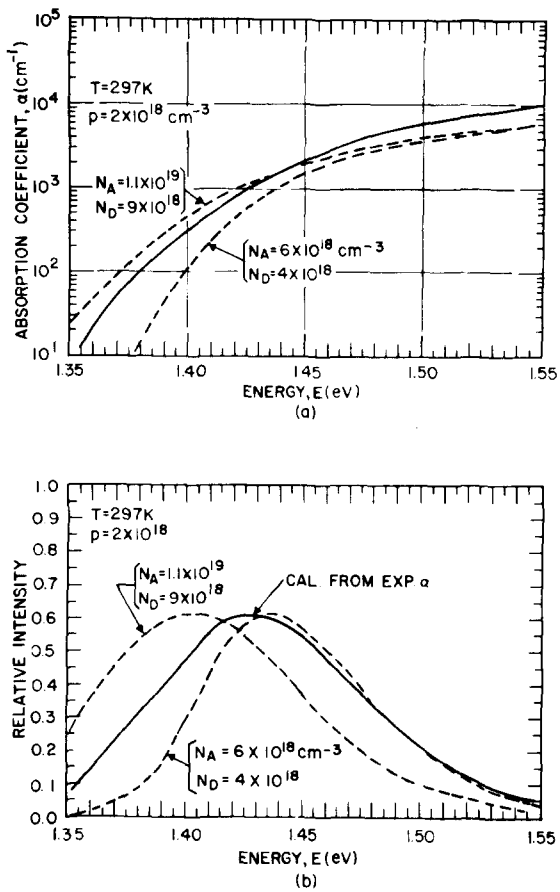

FIG. 7. (a) Comparison of the experimental and calculated absorption coefficients for closely compensated Si-doped GaAs. The effective energy gap used in the calculated absorption coefficient is taken from Eq. (15). (b) Comparison of the emission spectrum calculated with the experimental α in Eq. (14) and the spectrum calculated from the model for the indicated N_A and N_D.

TABLE III. Parameters for n-type GaAs samples.

n (cm^{-3})	Mobility ($cm^2/V\,sec$)	N_D (cm^{-3})	N_A (cm^{-3})
2×10^{18}	2660	2.5×10^{18}	5×10^{17}
3.3×10^{18}	2370	4.1×10^{18}	8×10^{17}
6.7×10^{18}	1900	8.4×10^{18}	1.7×10^{18}

and emission spectra are described in Table III. Comparison of these Hall mobilities with the Hall mobilities of uncompensated n-type GaAs[63] suggests that $N_D/N_A \approx 5.0$ for these samples. The values of N_D and N_A were assigned to give this N_D/N_A ratio. Comparison of the experimental absorption coefficient with the absorption coefficient obtained from the model of Sec. II does not result in as good agreement as for p-type material. Therefore, this part of Sec. III will only briefly consider n-type GaAs.

The absorption coefficients calculated from the model given in Sec. II are shown in Fig. 8(a) for $n = 2\times10^{18}$, 3.3×10^{18}, and 6.7×10^{18} cm^{-3}. The experimental absorption coefficients for the same free-electron concentrations are shown in Fig. 8(b) and were taken from Ref. 16 with the free-carrier absorption removed. The general features of the variation of α with n, such as the Burstein shift[64] and the flattening of the slope of α as n increases, are given by the calculated absorption coefficient. As for the p-type case, at high energies the calculated α is smaller than the experimental α, but the detailed shapes are not in as close agreement as for p-type GaAs.

Because the hole diffusion length for n-type GaAs for $n > 2\times10^{18}$ cm^{-3} is less than 1 μm,[59] the photoluminescent peak position and half-width should not be influenced very much by self-absorption. Therefore, the emission spectra calculated from the experimental absorption coefficient by Eq. (14) and calculated from the model of Sec. II should resemble the photoluminescent spectra. The emission spectra obtained from the experimental α using Eq. (14) tend to be ~0.010—0.020 eV higher than the photoluminescent peak position and 0.010 eV narrower in half-width. The emission spectra calculated from the model are as much as 0.050 eV lower in energy than the photoluminescent spectra and have a 0.030-eV larger half-width in the worst case at 6.7×10^{18} cm^{-3}.

With these differences, it is necessary to consider the accuracy of the experimental absorption coefficients. For $\alpha < 10^3$ cm^{-1}, the data in Ref. 16 were obtained by transmission measurements and are as accurate as for p-type GaAs which reconciles with the photoluminescence results. At higher absorption coefficients α was obtained by a Kramers-Kronig analysis[16] and may be less accurate for n- than p-type GaAs. However, the experimental α data of Fig. 8(b) differ somewhat from the data by Hill[4] or Hwang[13] at similar values of n. In addition, Hill's[4] and Hwang's[13] data do not exactly agree either. Therefore, the absorption coefficient for heavily doped n-type GaAs may be sample dependent. Sample-dependent absorption is generally observed for n-type GaP.[65] Melt-grown GaAs doped with Te, Se, or S has long been known to contain Te, Se, or S concentrations considerably in excess of the free-electron concentration,[66] with the excess impurity present as Ga_2Se_3 in the case of Se.[67] These precipitates do result in optical inhomogeneities,[68] but it is not clear how the optical transmission measurements of α will be influenced. These results suggest that transmission and photoluminescence measurements with the three-layered $Al_xGa_{1-x}As$-GaAs-$Al_xGa_{1-x}As$ structure[58] would be useful in reconciling these differences in the experimental α for n-type GaAs. Comparison could then be made between the spectra calculated from this measured α and the photoluminescence spectra to determine if α is due to band-to-band transistions only or is influenced by scattering from the precipitates.

IV. RADIATIVE RECOMBINATION PARAMETERS

Because of the difficulties with n-type GaAs, the radiative recombination parameters will only be considered for p-type GaAs. The quantity of interest is the radiative lifetime τ_r which requires the evaluation of the total thermal generation rate and the thermal equilibrium electron-hole density product $n_0 p_0$. The total thermal generation rate per unit volume,

$$G = \int_0^\infty \mathcal{G}(E)\,dE, \tag{16}$$

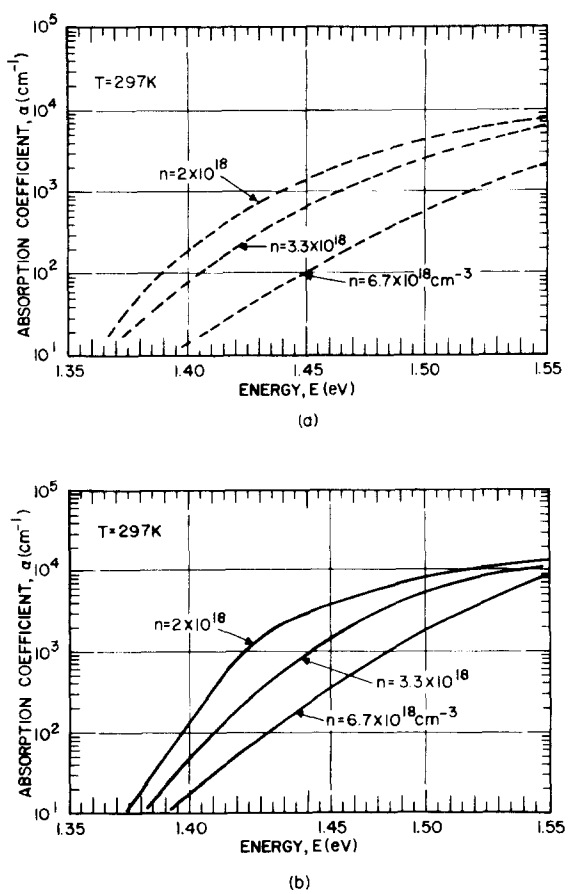

FIG. 8. (a) Absorption coefficient calculated for the indicated electron concentrations. The effective energy gap used in the calculated absorption coefficient is taken from Eq. (15). (b) Experimental absorption coefficient for the indicated electron concentrations (Ref. 16).

TABLE IV. Radiative recombination parameters for p-type GaAs at 297 K.

p (cm^{-3})	n_0p_0 (cm^{-6})	G (cm^{-3}/sec)		B ($10^{-10}cm^3$/sec)		τ_r (nsec)	
		Calc from expt α	Calc from model	Calc from expt α	Calc from model	Calc from expt α	Calc from model
1.2×10^{18}	6.8×10^{12}	2200	1300	3.2	1.9	2.6	4.4
2.4×10^{18}	8.1×10^{12}	2250	1400	2.8	1.7	1.5	2.4
1.6×10^{19}	1.2×10^{13}	2080	1100	1.7	0.9	0.37	0.7
Si-A	1.4×10^{13}		2800	3.8	2.0	1.3	2.5
Si—2×10^{18}	. . .	5490					
Si-B	3.4×10^{13}		6800	1.6	2.0	3.1	2.5

is the integral of the equilibrium spontaneous emission spectrum $\mathcal{J}(E)$, given by Eq. (14), calculated from the measured absorption coefficient $\alpha(E)$. The total radiative recombination rate is given by the familiar expressions[69,70]

$$R_r = Gnp/n_0p_0 = Bnp, \tag{17}$$

where n and p are the electron and hole concentrations for the excited material. When the excitation is sufficiently weak so that $p \approx p_0$, the radiative lifetime is given by[69,70]

$$\tau_r = (n - n_0)/R_r = 1/Bp, \tag{18}$$

with R_r given by Eq. (17) and $n \gg n_0$. It has not been possible to determine n_0p_0 experimentally, and therefore calculated values of $n_0p_0 = n_i^2/\gamma_n\gamma_p$ must be used, where n_i is the intrinsic carrier concentration in pure material and the γ's are activity coefficients.[71–73]

The values obtained for n_0p_0 from the model described in Sec. II are given in Table IV. For the parameters used here, $n_i^2 = 3.2\times10^{12}$ cm^{-6}. Note that for heavily doped p-type GaAs, $n_0p_0 > n_i^2$ and $\gamma_n\gamma_p < 1.0$. This result is in agreement with previous determinations of γ_p at high temperatures.[71,72] These values of n_0p_0, together with the absorption coefficient, are the quantities necessary for the evaluation of the radiative constant B and the radiative lifetime.

The total thermal generation rate G as calculated from the experimental absorption coefficient by Eqs. (14) and (16) is designated in Table IV as "calc. from expt α". The values of G calculated from the model of Sec. II are also given. The values of G obtained from the experimental absorption coefficient and from the model differ approximately by the same factor of 1.5–2.1 that was found for the experimental and calculated absorption coefficients. The radiative constant B is given by Eq. (17) and the radiative lifetime is given by Eq. (18). The radiative lifetimes for $p = 1.2\times10^{18}$, 2.4×10^{18}, and 1.6×10^{19} cm^{-3} are plotted in Fig. 9, and the values of B are listed in Table IV.

With the values of τ_r given in Table IV and Fig. 9 for heavily doped p-type GaAs, it is interesting to consider previous results for minority-carrier lifetime τ and diffusion length L_n. The over-all lifetime is given by

$$\tau = \tau_r\tau_{nr}/(\tau_{nr} + \tau_r), \tag{19}$$

where τ_{nr} is the nonradiative lifetime. Therefore, the minority-carrier lifetime cannot be longer than τ_r and becomes τ_r only for $\tau_r \ll \tau_{nr}$. For the minority-carrier diffusion length given by $L_n = (D_n\tau)^{1/2}$, and with the diffusivity related to the mobility μ as $D_n = \mu kT/q$, it is possible to relate L_n to τ. Lifetime values obtained in this way from the diffusion lengths of Ref. 59 are also shown in Fig. 9. The electron mobilities were assigned at each hole concentration by using the mobility obtained in an n-type sample of the same carrier concentration. Electron mobility as a minority carrier may be less than as a majority carrier, but is not expected to be greater than this value.[74] Therefore, actual lifetimes should be slightly less than the values assigned for these mobilities. At low concentrations, the lifetime is dominated by nonradiative recombination, while at high hole concentrations the calculated lifetimes and the values derived from diffusion length measurements are in reasonable agreement. The diffusion length measurements in Ref. 59 generally agree with the values obtained by others.[75–79] However, when either a scanning light spot[80] or a scanning electron beam[81] is used, the resulting lifetime values exceed the calculated values by a factor of ~10. This difficulty was described by van Opdorp *et al.*[82] as due to excited luminescence being absorbed and yielding a photocurrent contribution. Therefore, when the available experimental data are

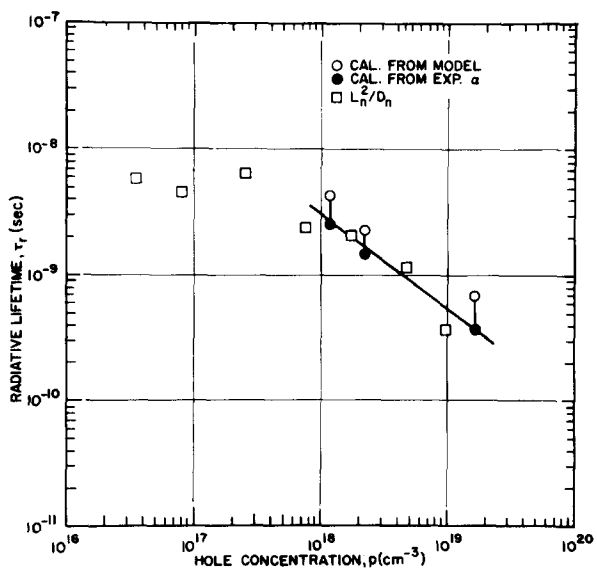

FIG. 9. Radiative lifetime as a function of the hole concentration at 297 K. The data shown by the squares are the lifetimes obtained from previous diffusion length measurements (Ref. 59).

considered, it appears that the numerical quantities summarized in Table IV and Fig. 9 are representative of the recombination constants for p-type GaAs.

V. DISCUSSION

In this section we consider the comparison of theory and experiment for the results presented above.

A. Magnitude of absorption

The most striking discrepancy between the measured and calculated values of the absorption coefficient of p-type GaAs is in the magnitude of the absorption coefficient at energies above the absorption edge. The experimental values exceed the calculated values by a factor 1.6 ± 0.1 in the energy range from 1.45 to 1.55 eV for the two less heavily doped samples, and by a factor near 2 for the sample with $p = 1.6 \times 10^{19}$ cm^{-3}. The corresponding factor is uncertain for the Si-doped sample because the degree of compensation is not known.

To examine the sensitivity of the results to changes in energy band parameters we used Kane's model for III-V semiconductors,[50] which does not include band tailing. The uncertainty in the calculated absorption associated with nonparabolicity, valence-band warping, and uncertainty in the values of the valence-band parameters[83-85] is estimated to be less than 20%. We therefore conclude that the cause of the discrepancy in α lies elsewhere, and is most likely due to Coulomb enhancement of the optical matrix element. Although such an enhancement is indicated by the present results, it would increase the calculated room-temperature threshold current density of semiconductor lasers by almost as large a factor, and would effect the comparison of theory[19] and experiment.[86,87] The need for a matrix-element enhancement to reconcile theory and experiment for semiconductor lasers was pointed out by Hwang,[88] and related calculations have been carried out by several authors.[30-32] Calculations of the optical matrix element which include heavy-doping effects as well as Coulomb effects must be carried out before these problems can be resolved.

B. Effective energy gap shrinkage

The effective reduction of the energy gap in heavily doped semiconductors has been considered by many authors, and we will not attempt to give a complete account of the previous work. For p-type semiconductors, the exchange contribution to the energy gap shrinkage as measured at the Fermi level is[89,90]

$$\mu_x = -(e^2/4\pi^2\epsilon)(3\pi^2 p)^{1/3}\Psi, \tag{20}$$

where ϵ is the permittivity of GaAs and Ψ is a correction factor which depends on the ratio of light- and heavy-hole masses. For the values used here, $\Psi = 0.73$, and Eq. (20) gives

$$\mu_x \text{ (eV)} = -8 \times 10^{-9}[p \text{ (cm}^{-3})]^{1/3}. \tag{21}$$

We evaluate the exchange energy at the Fermi level because the absorption in heavily doped semiconductors is sensitive to the position of the Fermi level.

The magnitude of the effective energy gap shrinkage is determined by comparing the calculated absorption coefficient curve with the corresponding experimental curve and finding the energy shift which gives the best fit. Since the calculation includes both degeneracy effects (Burstein-Moss shift) and band-tailing effects, one may hope that a reliable value of the gap shrinkage can be obtained. The results in Fig. 6 show that the energy gap shrinkage can be fitted by Eq. (15), which exceeds the value from exchange effects by about a factor 2.

Rimbey and Mahan[91] have calculated an additional contribution of the energy gap shrinkage caused by interaction of the carriers with the ionized impurities. A simple form of their result is

$$\mu_I^{TF} = -0.61 E_d / r_s^{1/2}, \tag{22}$$

where $E_d = m^* e^4/32\pi^2\epsilon^2\hbar^2$ is the effective Ryberg, $r_s a^* = (3/4\pi p)^{1/3}$, and a^* is the effective Bohr radius used in Eq. (8). For the values used here this gives

$$\mu_I^{TF} \text{ (eV)} = -1.2 \times 10^{-5}[p \text{ (cm}^{-3})]^{1/6}. \tag{23}$$

Rimbey and Mahan did not explicity include compensation effects.

One other effect of carriers on the energy gap is the interaction with optical phonons. In a polar material like GaAs, the polaron binding energy is

$$E_p = -\alpha\hbar\omega_l = -(e^2/4\pi\epsilon_0)(\kappa_\infty^{-1} - \kappa_s^{-1})(m^*\omega_l/2\hbar)^{1/2}, \tag{24}$$

where κ_∞ and κ_s are the optical and static dielectric constants, respectively, and $\omega_l/2\pi$ is the longitudinal optical frequency. If we use $\hbar\omega_l = 0.037$ eV,[92] $\kappa_\infty = 10.9$, $\kappa_s = 13$, and $m^* = 0.55m$, we find $\alpha = 0.21$ and $E_p = -0.0078$ eV. This energy is already included in the experimentally determined energy gap for relatively pure samples. As carriers are added to the system, the polaron binding energy decreases[93,94] and there is an effective increase of the gap. Its magnitude has been estimated for PbSe by Asbeck.[94] Because of the degenerate valence-band structure and the impurity effects, a corresponding calculation will be more difficult for GaAs. We expect that this effect opposes the gap reductions predicted by Eqs. (20) and (22), but is smaller in magnitude.

We believe that the present method of estimating the shrinkage of the effective energy gap from comparison of calculated and measured absorption curves is more reliable than methods which use only a single value of the absorption coefficient and generally ignore band-tailing effects. Comparison of the experimental and theoretical values of the effective energy gap shrinkage cannot be made until the correlation energy is included. The calculation is similar to that used for electron-hole drops,[89,95,96] but should include doping effects.

C. Band tailing

The experimental results presented here show considerably more band tailing than do the calculated values for absorption coefficients smaller than about 300 cm^{-1}. There are several possible reasons for this discrepancy. One is that the samples contain a higher concentration of charged impurities than estimated in Sec. III, where a compensation ratio $N_A/N_D = 5$ was deduced.

Another is that the Gaussian model used in the calculation ignores the asymmetry present in the potential fluctuations.[44] This asymmetry will enhance the density of states in the valence band tail while decreasing the density of states in the conduction band tail. The net effect on the absorption is an increase in the width of the absorption tail, in qualitative agreement with experiment.

The discrepancy between theory and experiment can also be attributed in part to the Gaussian fit to the Halperin-Lax density of states which we described in Sec. II, because the Gaussian Kane function falls off too rapidly in the band tail. Carrier-carrier interactions[32,97] and phonon effects[98] also lead to a broadening of the band edge, although such effects should be relatively less important in heavily doped samples than in more lightly doped samples. The relative importance of each of these mechanisms is of some interest, and additional calculations to estimate their magnitude in heavily doped samples would be useful.

D. *n*-type GaAs

The calculated absorption coefficients for *n*-type GaAs in Fig. 8 reproduce the general trends of the experimental curves shown there, but are sufficiently different in shape that we do not attempt a detailed comparison for *n*-type material. One possible reason for the poorer agreement is that the transitions in *n*-type material are more sensitive to the valence band tail, where the approximations used here are particularly weak.

E. Radiative lifetime

The radiative lifetime τ_r is closely tied to the optical absorption, as discussed in Sec. IV, and can also be measured independently. The lifetime τ can be deduced from the measured diffusion length and an estimated mobility, as discussed above, or it can be measured directly from the rate of decay of luminescence. The radiative lifetime is found from τ and the internal quantum efficiency η_q by using $\tau_r = \tau/\eta_q$. From Hwang's result[99] for τ and η_q, a value for the radiative recombination constant B from Eq. (17) of 2.3×10^{-11} cm^3/sec can be deduced for a Te-doped sample with $n = 2\times10^{17}$ cm^{-3}. Imai *et al.*[100] estimated τ_r as 0.12 ± 0.02 μsec by measuring η_q and τ for a sample with $n = 1.2\times10^{17}$ cm^{-3}, which gives $B = 7\times10^{-11}$ cm^3/sec. This difference in B by a factor of 3 for similar samples illustrates the numerous difficulties in the experimental assignment of τ_r and B.

Acket *et al.*[79] obtained $\tau = 1/B'p$, with $B' = 6.4\times10^{-11}$ cm^3/sec, for the total lifetime in Ge-doped GaAs with hole concentrations between 2×10^{18} and 8×10^{18} cm^{-3}. Hwang and Dyment[101] found $B' = 1.3\times10^{-10}$ cm^3/sec from an analysis of lasing delays in liquid-phase epitaxial GaAs with 2×10^{17}–3×10^{19} Ge acceptors per cm^3, and Namizaki *et al.*[102] found $B' = 9\times10^{-11}$ cm^3/sec from a similar analysis for a Si-doped active layer with $p \approx 2\times10^{17}$ cm^{-3}.

The lifetime deduced from the measured absorption and the *np* product using detailed balance, as described in Sec. IV, is sensitive to errors in the band parameters. The conduction-band and valence-band masses used in our calculation are thought to be correct within 10%. Our estimated uncertainty of 0.003–0.005 eV in the effective energy gap shrinkage leads to an uncertainty of about 20% in the equilibrium *np* product at room temperature. We estimate, therefore, that the effective recombination constant B and the radiative lifetime which we obtain in Sec. IV are correct within 25%. The experimental lifetime values in Fig. 9 will be lower than the radiative lifetime if nonradiative recombination is significant. The comparison of our estimated values with those deduced from the diffusion length is somewhat better than these considerations would lead us to expect.

At high carrier concentrations the radiative lifetime of injected electrons is expected to approach a minimum lifetime given by[103]

$$\tau_{\min} = m^2c^3\hbar^2\pi\epsilon_0/4\bar{n}e^2E_g|M_b|^2. \tag{25}$$

For electrons in GaAs this gives $\tau_{\min} = 0.3$ nsec. If the Coulomb enhancement factor discussed above applied throughout, then the minimum lifetime would be reduced to ≈ 0.2 nsec. The values in Fig. 9 suggest that the minimum lifetime is approached for the highest hole concentration considered here.

VI. CONCLUSIONS

The experimental and calculated emission spectra were compared for heavily doped GaAs with carrier concentrations in excess of $\sim 1\times10^{18}$ cm^{-3}. These comparisons demonstrated the necessity of including both the band tails for the density of states and an energy-dependent matrix element in the model for the optical spectra. For *p*-type GaAs this model agrees closely with the shape of the absorption coefficient and changes with increasing hole concentration as observed experimentally. However, at low energies the calculated absorption coefficient decreases more rapidly than observed experimentally, and at high energies the absolute absorption strength is too weak by a factor of approximately 1.5–2.1. This discrepancy is believed to be due to Coulomb enhancement of the optical matrix element, which has not been included in the model. The calculated and experimental spontaneous emission spectral shapes agreed within ±0.001 eV in half-width and 0.01 eV in peak position. The agreement was not as close for *n*-type GaAs, but the calculated absorption spectra varied with carrier concentration in the same manner as observed experimentally.

Several numerical quantities were obtained by the comparison of the experimental and calculated spectra. The concentration dependence of the energy gap was obtained by the best fit between the measured and calculated absorption edges and was found to decrease as $1.6\times10^{-8}p^{1/3}$, where the energy is in eV and the hole concentration is in cm^{-3}. The good agreement between the calculated and the measured spectral shapes demonstrates that the densities of states used in the model are representative of heavily doped GaAs. With these densities of states, the concentration-dependent thermal-equilibrium electron-hole products n_0p_0 were calculated. It has not been possible to obtain these quan-

tities by experiment only. The effective recombination constant B decreases from about 3.2×10^{-10} cm^3/sec when $p=1.2\times10^{18}$ cm^{-3} to 1.7×10^{-10} cm^3/sec when $p=1.6\times10^{19}$ cm^{-3}. The radiative lifetime decreases from 2.6 to 0.37 nsec over this same concentration range. These lifetimes limit the minority-carrier diffusion length that may be achieved at high impurity concentrations.

ACKNOWLEDGMENTS

The authors are indebted to P.M. Asbeck, W.F. Brinkman, T. Kamiya, P. Lawaetz, and R.A. Stradling for helpful discussions and correspondence.

[1]I. Kudman and T. Seidel, J. Appl. Phys. **33**, 771 (1962).
[2]M.I. Nathan, G. Burns, S.E. Blum, and J.C. Marinace, Phys. Rev. **132**, 1482 (1963).
[3]D.A. Cusano, Solid State Commun. **2**. 353 (1964).
[4]D.E. Hill, Phys. Rev. **133**, A866 (1964).
[5]W.J. Turner and W.E.Reese, J. Appl. Phys. **35**, 350 (1964).
[6]J.I. Pankove, Phys. Rev. **140**, A2059 (1965).
[7]V.S. Bagaev, Y.N. Berozashvili, L.V. Keldysh, A.P. Shotov, B.M. Vul, and E.I. Zavaritaskaya, in *Radiative Recombination in Semiconductors* (Dunod, Paris, 1965), p. 149.
[8]M.I. Nathan and T.N. Morgan, in *Physics of Quantum Electronics*, edited by P.L. Kelley, B. Lax, and P.E. Tannenwald (McGraw-Hill, New York, 1966), p. 478.
[9]J.I. Pankove, J. Appl. Phys. **39**, 5368 (1968).
[10]B. Tuck, J. Phys. Chem. Solids **29**, 615 (1968).
[11]H.C. Casey, Jr. and R.H. Kaiser, J. Electrochem. Soc. **114**, 149 (1967).
[12]H. Kressel and H. Nelson, J. Appl. Phys. **40**, 3720 (1969).
[13]C.J. Hwang, J. Appl. Phys. **40**, 3731 (1969).
[14]P.D. Southgate, J. Phys. Chem. Solids **31**, 55 (1970).
[15]Zh.I. Alferov, V.M. Andreev, D.Z. Garbuzov, and M.K. Trukan, Fiz. Tekh. Poluprov. **6**, 2015 (1972) [Sov. Phys.-Semicond. **6**, 1718 (1973)].
[16]H.C. Casey, Jr., D.D. Sell, and K.W. Wecht, J. Appl. Phys. **46**, 250 (1975).
[17]See also E.W. Williams and H.B. Bebb, in *Semiconductors and Semimetals*, edited by R.K. Willardson and A.C. Beer (Academic, New York, 1972), Vol. 8, pp. 321—392.
[18]F. Stern, in *Laser Handbook*, edited by F.T. Arecchi and E.O. Schulz-Dubois (North-Holland, Amsterdam, 1972), Vol. 1, p. 425.
[19]F. Stern, IEEE J. Quantum Electron. **QE-9**, 290 (1973).
[20]F. Stern, Phys. Rev. B **3**, 3559 (1971).
[21]F. Stern, Phys. Rev. B **3**, 2636 (1971).
[22]L.V. Keldysh and G.P. Proshko, Fiz. Tverd. Tela. **5**, 3378 (1963) [Sov. Phys.-Solid State **5**, 2481 (1964)].
[23]V.L. Bonch-Bruevich, Phys. Status Solidi **42**, 35 (1970).
[24]T. Lukes and K.T.S. Somaratna, J. Phys. C **3**, 2044 (1970).
[25]B.I. Shklovskii and A.L. Efros, Zh. Eksp. Teor. Fiz. **59**, 1343 (1970) [Sov. Phys.-JETP **32**, 733 (1971)].
[26]E.V. Burtsev, Phys. Status Solidi B **51**, 241 (1972).
[27]H. Van Cong and G. Mesnard, Phys. Status Solidi B **52**, 553 (1972).
[28]A.G. Aleksanian, I.A. Poluektov, and Yu.M. Popov, IEEE J. Quantum Electron. **QE-10**, 297 (1974).
[29]R.J. Elliott, Phys. Rev. **108**, 1384 (1957).
[30]G.D. Mahan, Phys. Rev. **153**, 882 (1967).
[31]J.D. Dow, D.L. Smith, and F.L. Lederman, Phys. Rev. B **8**, 4612 (1973).
[32]W.F. Brinkman and P.A. Lee, Phys. Rev. Lett. **31**, 237 (1973).
[33]See, for example, G. Lasher and F. Stern, Phys. Rev. **133**, A553 (1964).
[34]P.D. Southgate, J. Appl. Phys. **40**, 5333 (1969).
[35]D. Redfield, J.P. Wittke, and J.I. Pankove, Phys. Rev. B **2**, 1830 (1970).
[36]V.V. Osipov, Fiz. Tekh. Poluprov. **7**, 2106 (1973) [Sov. Phys.-Semicond. **7**, 1405 (1974)].
[37]H.C. Casey, Jr. and R.Z. Bachrach, J. Appl. Phys. **44**, 2295 (1973).
[38]E.O. Kane, Phys. Rev. **131**, 79 (1963).
[39]V.L. Bonch-Bruevich, in *Semiconductors and Semimetals*, edited by R.K. Willardson and A.C. Beer (Academic, New York, 1966), Vol. 1, p. 101.
[40]B.I. Halperin and M. Lax, Phys. Rev. **148**, 722 (1966).
[41]J. Zittartz and J.S. Langer, Phys. Rev. **148**, 741 (1966).
[42]B.I. Shklovskii and A.L. Efros, Fiz. Tekh. Poluprov. **4**, 305 (1970) [Sov. Phys. Semicond. **4**, 249 (1970)].
[43]M. Saitoh and S.F. Edwards, J. Phys. C **7**, 3937 (1974).
[44]T.N. Morgan, Phys. Rev. **139**, A343 (1965).
[45]V.L. Bonch-Bruevich, Dokl. Akad. Nauk SSSR **189**, 505 (1969) [Sov. Phys.-Dokl. **14**, 1101 (1970)].
[46]F. Stern, in *Conduction in Low-Mobility Materials*, edited by N. Klein, D.S. Tannhauser, and M. Pollak (Taylor and Francis, London, 1971), p. 211.
[47]C.J. Hwang, Phys. Rev. B **2**, 4117 (1970).
[48]C.J. Hwang, J. Appl. Phys. **41**, 2668 (1970).
[49]R. Eymard and G. Duraffourg, J. Phys. D **6**, 66 (1973).
[50]E.O. Kane, J. Phys. Chem. Solids **1**, 249 (1957).
[51]D.M. Eagles, J. Phys. Chem. Solids **16**, 76 (1960).
[52]F. Stern, J. Non-cryst. Solids **4**, 256 (1970).
[53]F. Ermanis and K. Wolfstirn, J. Appl. Phys. **37**, 1963 (1966).
[54]D.L. Malm (private communication).
[55]J.K. Kung and W.G. Spitzer, J. Appl. Phys. **45**, 2254 (1974).
[56]W. van Roosbroeck and W. Shockley, Phys. Rev. **94**, 1558 (1954).
[57]E.W. Williams and R.A. Chapman, J. Appl. Phys. **38**, 2547 (1967).
[58]D.D. Sell and H.C. Casey, Jr., J. Appl. Phys. **45**, 800 (1974).
[59]H.C. Casey, Jr., B.I. Miller, and E. Pinkas J. Appl. Phys. **44**, 1281 (1973).
[60]D.D. Sell, H.C. Casey, Jr., and K.W. Wecht, J. Appl. Phys. **45**, 2650 (1974).
[61]K.L. Ashley and H.A. Strack, in *Proceedings of the Second International Symposium on GaAs* (Institute of Physics and Physical Society, London, 1969), p. 123.
[62]E. Pinkas, B.I. Miller, I. Hayashi, and P.W. Foy, J. Appl. Phys. **43**, 2827 (1972).
[63]D.L. Rode and S. Knight, Phys. Rev. B **3**, 2534 (1971).
[64]E. Burstein, Phys. Rev. **93**, 632 (1954).
[65]R.W. Dixon (private communication).
[66]L.J. Vieland and I. Kudman, J. Phys. Chem. Solids **24**, 437 (1963).
[67]M.S. Abrahams, C.J. Buiocchi, and J.J. Tietjen, J. Appl. Phys. **38**, 760 (1967).
[68]M.E.Drougard, J. Appl. Phys. **37**, 1858 (1966).
[69]Y.P. Varshni, Phys. Status Solidi **19**, 459 (1967).
[70]R.N. Hall, Proc. Inst. Elec. Eng. B **106**, 923 (1959).
[71]M.B. Panish and H.C. Casey, Jr., J. Phys. Chem. Solids **28**, 1673 (1967).
[72]H.C. Casey, Jr., M.B. Panish, and L.L. Chang, Phys. Rev. **162**, 660 (1967).
[73]C.J. Hwang and J.R. Brews, J. Phys. Chem. Solids **32**, 837 (1971).
[74]M.B. Prince, Phys. Rev. **92**, 681 (1953).
[75]L.W. James, J.L. Moll, and W.E. Spicer, in Ref. 61, p. 230.
[76]H. Schade, H. Nelson, and H. Kressel, Appl. Phys. Lett. **18**, 121 (1971).
[77]M.S. Abrahams, C.J. Buiocchi, and B.F. Williams, Appl. Phys. Lett. **18**, 220 (1971).
[78]T. Kawakami and K. Sugiyama, Jpn. J. Appl. Phys. **12**, 151 (1973).
[79]G.A. Acket, W. Nijman, and H.'t Lam, J. Appl. Phys. **45**, 3033 (1974).
[80]K.L. Ashley, D.L. Carr, and R. Ramano-Moran, Appl. Phys. Lett. **22**, 23 (1973).
[81]M. Ettenberg, H. Kressel, and S.L. Gilbert, J. Appl. Phys. **44**, 827 (1973).

[82]C. van Opdorp, R.C. Peters, and M. Klerk, Appl. Phys. Lett. **24**, 125 (1974).
[83]R.A. Stradling, Proceedings of the International Conference on High Magnetic Fields, Grenoble, 1974 (unpublished).
[84]P. Lawaetz (private communication).
[85]N.D. Lipari, M. Altarelli, and R. Dingle, Solid-State Commun. **16**, 1189 (1975).
[86]H. Kressel and H.F. Lockwood, Appl. Phys. Lett. **20**, 175 (1972).
[87]B.W. Hakki and T.L. Paoli, J. Appl. Phys. **46**, 1299 (1975).
[88]C.J. Hwang, 1972 IEEE Semiconductor Laser Conference (unpublished).
[89]M. Combescot and P. Nozieres, J. Phys. C **5**, 2369 (1972), Eq. (26).
[90]We have multiplied the result in Ref. 89 by $1/4\pi$ to convert to mks units and by a factor 5/3 to convert from the total exchange energy per electron to the exchange energy of an electron at the Fermi level. See, for example, W. Kohn and L.J. Sham, Phys. Rev. **140**, A1133 (1965).
[91]P.R. Rimbey and G.D. Mahan, Phys. Rev. B **10**, 3419 (1974).
[92]M. Hass and B.M. Henvis, J. Phys. Chem. Solids. **23**, 1099 (1962).
[93]G.D. Mahan, in *Polarons in Ionic Crystals and Polar Semiconductors*, edited by J.F. Devreese (North-Holland, Amsterdam, 1972), p. 553.
[94]P.M. Asbeck, Ph.D. thesis (Massachusetts Institute of Technology, Cambridge, Mass., 1975) (unpublished).
[95]W.F. Brinkman and T.M. Rice, Phys. Rev. B **7**, 1508 (1973).
[96]P. Vashishta, S.G. Das, and K.S. Singwi, Phys. Rev. Lett. **33**, 911 (1974).
[97]P.T. Landsberg, Solid-State Electron. **10**, 513 (1967).
[98]See, for example, J.D. Dow and D. Redfield, Phys. Rev. B **5**, 594 (1972).
[99]C.J. Hwang, Phys. Rev. B **6**, 1355 (1972).
[100]H. Imai, T. Kuriyama, T. Kamiya, and H. Yanai, Annual Convention of the Japan Society for Applied Physics, April, 1974 (unpublished). The sample was grown by vapor phase epitaxy and was not intentionally doped, but is thought to contain Si.
[101]C.J. Hwang and J.C. Dyment, J. Appl. Phys. **44**, 3240 (1973).
[102]H. Namizaki, H. Kan, M. Ishii, and A. Ito, Appl. Phys. Lett. **24**, 486 (1974).
[103]W.P. Dumke, Phys. Rev. **132**, 1998 (1963).